



OPEN

Design and characterization of an urea-bridged PMO supporting Cu(II) nanoparticles as highly efficient heterogeneous catalyst for synthesis of tetrazole derivatives

Ehsan Valiey & Mohammad G. Dekamin✉

In this work, a new periodic mesoporous organosilica with urea-bridges produced by the reaction of (3-aminopropyl)triethoxysilane and toluene-2,4-diisocyanate (APS-TDU-PMO) is introduced. The obtained APS-TDU-PMO was found to be an appropriate support for loading of Cu(II) nanoparticles to afford supramolecular Cu@APS-TDU-PMO nanocomposite. Uniformity and mesoporosity of both synthesized nanomaterials including APS-TDU-PMO and Cu@APS-TDU-PMO were proved by different spectroscopic, microscopic or analytical techniques including FTIR, EDX, XRD, FESEM, TEM, BET, TGA and DTA. Furthermore, the prepared Cu@APS-TDU-PMO nanomaterial was also used, as a heterogeneous and recyclable catalyst, for the synthesis of tetrazole derivatives through cascade condensation, concerted cycloaddition and tautomerization reactions. Indeed, the main advantages of this Cu@APS-TDU-PMO is its simple preparation and high catalytic activity as well as proper surface area which enable it to work under solvent-free conditions. Also, the introduced Cu@APS-TDU-PMO heterogeneous catalyst showed good stability and reusability for six consecutive runs to address more green chemistry principles.

Mesoporous silica nanomaterials (MSNs) are widely used in material science for various applications as well as special blocks for making various valuable assemblies. MSNs have been extensively studied and used for applications in diverse fields including catalysis, ion exchange, adsorption, chromatography, molecular sieving, CO₂ capture and even as templates for synthetic conductive carbon nanowires^{1–22} due to their special properties such as large specific surface, high pore volume, uniform and tunable pores, high stability, and low cost^{23–30}. Among different MSNs, periodic mesoporous organosilicas (PMOs) have received significant research interest in recent years. PMOs are hybrid porous materials with high surface area and large porosity obtained by sol–gel method from an organo-bridged alkoxysilane in the presence of a surfactant, which were first reported in 1999^{31–44}. The porous framework of PMOs is created by organic functional groups covalently binding to siloxane domains. In contrary to SBA-15 and MCM-41 which can only be functionalized at their surfaces by the grafting method^{45,46}, different organic functionalities of the organic-bridged silica precursors can be included in the silica framework^{47–49}. PMOs have some advantages over mesoporous silica materials including mechanical stability, hydrophobic pore wall, and high concentration of organic functional group in the framework, which have led to their applications in different fields such as hydrophobic drug carriers⁵⁰, adsorbents^{51,52}, biological/biomedical supports⁵³, optical applications⁵⁴, solid chromatographic phases⁵⁵ and catalysis^{44,56–60}.

Nowadays, developing of more efficient catalytic systems for the synthesis and manufacturing of both fine and bulk chemicals is in the focal point of academic as well as industrial research groups^{61–63}. new commercial applications, while environmental legislation created market pull to use catalysis to meet the new regulatory standards. As we move forward into the new century, we continue to see market pull from growing interests in biomass, sustainability, emissions control, and energy. due to It is essential to use suitable catalytic systems for

Pharmaceutical and Heterocyclic Compounds Research Laboratory, Department of Chemistry, Iran University of Science and Technology, Tehran 16846-13114, Iran. ✉email: mdekamin@iust.ac.ir

the preparation of very important medically and ecologically compounds^{64,65}. It is essential to use suitable catalytic systems for the preparation medically and ecologically very important compounds^{64,65}. Therefore, catalytic systems can be used for these purposes. The catalytic system consists of homogeneous and heterogeneous types. Also, heterogeneous catalysts have received more attention due to their many advantages such as easy separation from the reaction mixture, recyclability and subsequent reusability as well as less contamination in the final product^{66,67}. In this context, nanomaterials demonstrate appropriate selectivity in activity and shape due to their finely porous structure and high surface area⁶⁸. Also, by incorporation of acid and base centers as well as transition metallic species, they can be used in many organic transformations including acid or base-catalyzed reactions, oxidation, C–C coupling reactions, C–H activation, etc. to afford simple or complex molecules in both bulk and fine chemicals synthesis^{69–73}. Among the various metal nanoparticles, copper nanoparticles are of particular importance due to their high conductivity and natural abundance, easy access, low cost, and tremendous copper potential to replace precious metals such as palladium, platinum, gold, or silver. Indeed, immobilization of copper(II) species on organic and inorganic supports bearing appropriate ligands is one of the best methods for the production of heterogeneous catalytic systems with high stability, activity, and loading of active centers^{74–76}. Therefore, catalytic systems can be used for these purposes. The catalytic system consists of homogeneous and heterogeneous types. Also, heterogeneous catalysts have received more attention due to their many advantages such as easy separation from the reaction mixture, recyclability and subsequent reusability as well as less contamination in the final product^{66,67}. In this context, nanomaterials demonstrate appropriate selectivity in activity and shape due to their finely porous structure and high surface area⁶⁸. Also, by incorporation of acid and base centers as well as transition metallic species, they can be used in many organic transformations including acid or base-catalyzed reactions, oxidation, C–C coupling reactions, C–H activation, etc. to afford simple or complex molecules in both bulk and fine chemicals synthesis^{69–73,77,78}. Among the various metal nanoparticles, copper nanoparticles are of particular importance due to their high conductivity and natural abundance, easy access, low cost, and tremendous copper potential to replace precious metals such as palladium, platinum, gold, or silver. Indeed, immobilization of copper(II) species on organic or inorganic supports bearing appropriate ligands is one of the best methods for the production of heterogeneous catalytic systems with high stability, activity, and loading of active centers^{74–76}.

Due to the use of copper complexes in various chemical reactions such as hydroboration of alkenes^{79,80}, β -boration of α,β -unsaturated esters⁸¹, direct addition of terminal alkynes to imines^{82,83}, alkyne-azide cycloaddition^{84,85} and allylic alkylation reactions⁸⁶, special attention has been paid to copper complexes as catalysts for these reactions. Furthermore, the Cu(I)-assisted click chemistry (CuACC) of azide–nitrile cycloaddition for synthesis of corresponding heterocyclic compounds, namely tetrazole derivatives, has received much attention in recent years^{87–91}. Tetrazole derivatives are an important class of nitrogen-rich heterocyclic nucleus with significant applications in the medicinal chemistry. Indeed, tetrazole moiety serves as a useful pharmacophore in brand names including Lasortan, Irbesartan, and Tomelukast medications, which are used to treat high blood pressure, heart failure, diabetic kidney or asthma diseases. Furthermore, this pharmacophore is widely used in drug design studies as an appropriate isostere of carboxylic acid functional group^{92–99}. In addition, application of tetrazole derivatives as important widespread compounds in synthetic organic chemistry^{100,101}, catalysis and energetic applications¹⁰², materials chemistry¹⁰³, and as ligands in coordination chemistry¹⁰⁴ have led to the development of various efficient synthetic methods. Tetrazole derivatives are most commonly synthesized by [3 + 2] cycloaddition reaction of the corresponding azide and nitrile moieties^{105–112}. Therefore, attempts for the production of tetrazole derivatives through new methods have led to the use of 2-benzylidenemalononitrile and sodium azide along these lines^{113,114}. In continuation of interest to develop new PMOs or their assemblies and exploring their catalytic activities^{21,22,30,59,60,114}, this paper reports the synthesis of novel periodic mesoporous organosilica by the reaction of amino group of (3-aminopropyl)triethoxysilane and toluene-2,4-diisocyanate, namely APS-TDU-PMO, with walls having urea bridges for Cu nanoparticles loading (Cu@APS-TDU-PMO, **1**). Furthermore, the Cu@APS-TDU-PMO was used as a highly efficient and recoverable nanoreactor for the synthesis of tetrazole derivatives **5** via three-component addition of aldehydes (**2**), malononitrile (**3**), and sodium azide (**4**) (Fig. 1).

Results and discussion

The prepared Cu@APS-TDU-PMO nanomaterial (**1**) was characterized by Fourier transform Infrared (FTIR), thermal gravimetric analysis (TGA), differential thermal analysis (DTA), field emission scanning electron microscopy (FESEM), transmission electron microscopy (TEM), energy-dispersive X-ray (EDX), X-ray powder diffraction (XRD), and Brunauer–Emmett–Teller (BET) surface area analytical methods or techniques. The FTIR spectrum of both new APS-TDU-PMO and Cu@APS-TDU-PMO (**1**) are shown in Fig. 2. The broad absorption band at 3414 cm^{-1} is attributed to both N–H and O–H bonds stretching vibrations. Furthermore, two sharp absorption signals at 2928 cm^{-1} and 2862 cm^{-1} are assigned to the asymmetric and symmetric stretching vibration of aliphatic C–H bonds, respectively. On the other hand, the absorption bands at 1682 cm^{-1} and 1654 cm^{-1} correspond to C=O bond stretching vibration of the urea moiety in the structure of APS-TDU-PMO and Cu@APS-TDU-PMO (**1**). Furthermore, the band at 1544 cm^{-1} can be assigned to the stretching vibration of the aromatic C=C bonds. Also, two absorption bands at 1192 cm^{-1} and 1092 cm^{-1} are related to the Si–O–Si bonds (Fig. 2a). Interestingly, the absorption band of Cu–N chelation is clearly observed at the range of 800–700 cm^{-1} (Fig. 2b).

On the other hand, TGA and DTA curves of the Cu@APS-TDU-PMO (**1**) in Fig. 3 shows that the slight weight loss between 50 and 270 °C can be assigned to the elimination of adsorbed solvent or water molecules on its surface as well as degradation of small amounts of the unextracted surfactant (P123). Also, the weight loss between 270 and 460 °C is attributed to the decomposition of the urea bridges in the Cu@APS-TDU-PMO (**1**)

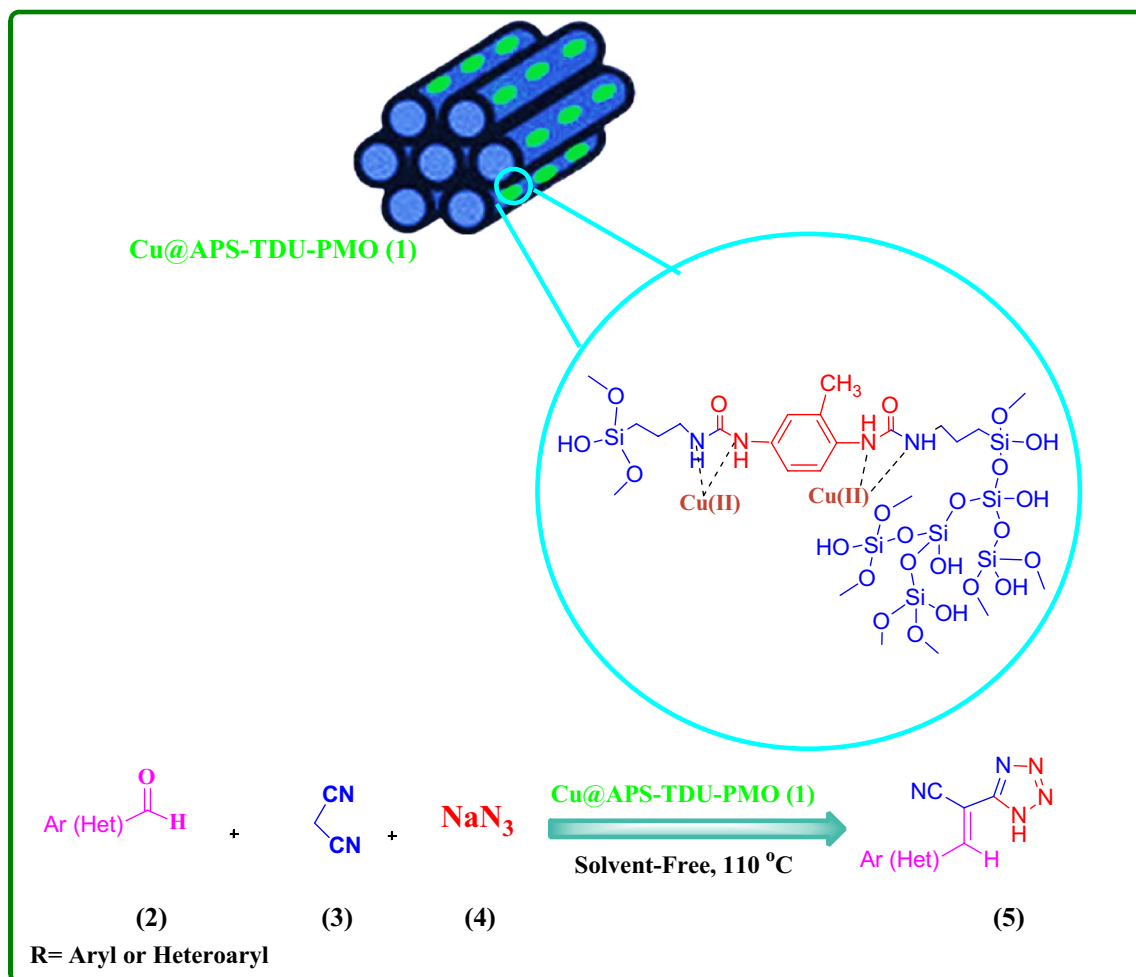


Figure 1. Schematic structure of the Cu@APS-TDU-PMO nanoreactor (1) for the three-component condensation of aldehydes (2a–i), malononitrile (3), and sodium azide (4).

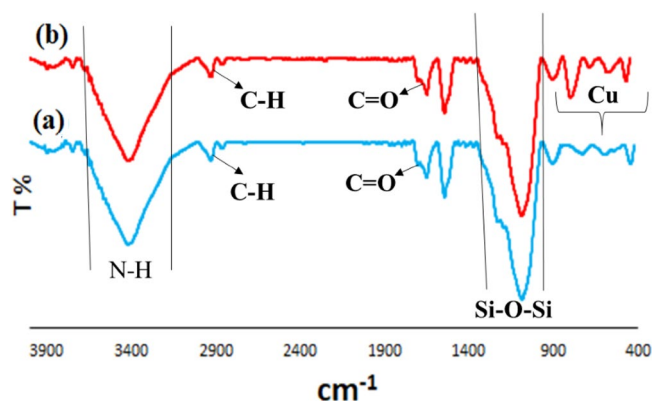


Figure 2. FTIR spectra of the APS-TDU-PMO (a) and Cu@APS-TDU-PMO (1, b).

structure. On the other hand, the last step of weight loss between 460 and 800 °C is due to condensation of the silanols to siloxanes in the structure of Cu@APS-TDU-PMO nanomaterial (1).

Furthermore, FESEM and TEM images show that the Cu@APS-TDU-PMO nanomaterial (1) is composed of a large number of interwoven rods with 41–59 nm in width (Fig. 4). It can also be seen that the morphology of PMO was mostly preserved after deposition of Cu nanoparticles. TEM images also demonstrate the uniform arrangement of mesopores and tubular mesochannels in the Cu@APS-TDU-PMO (1) structure (Fig. 4b).

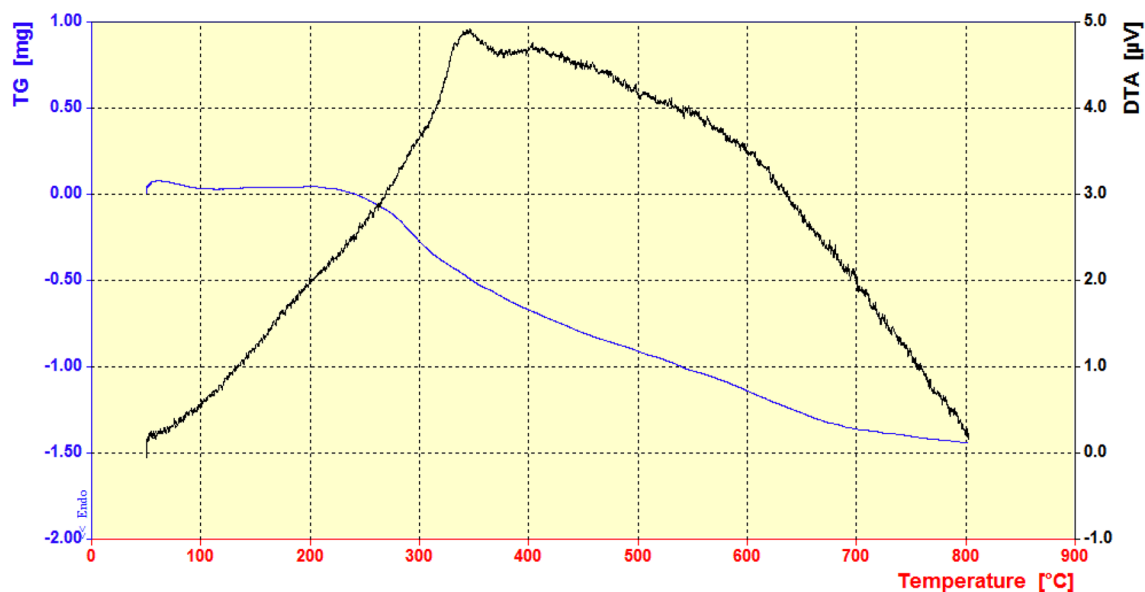


Figure 3. TGA and DTA curves of the Cu@APS-TDU-PMO nanomaterial (1).

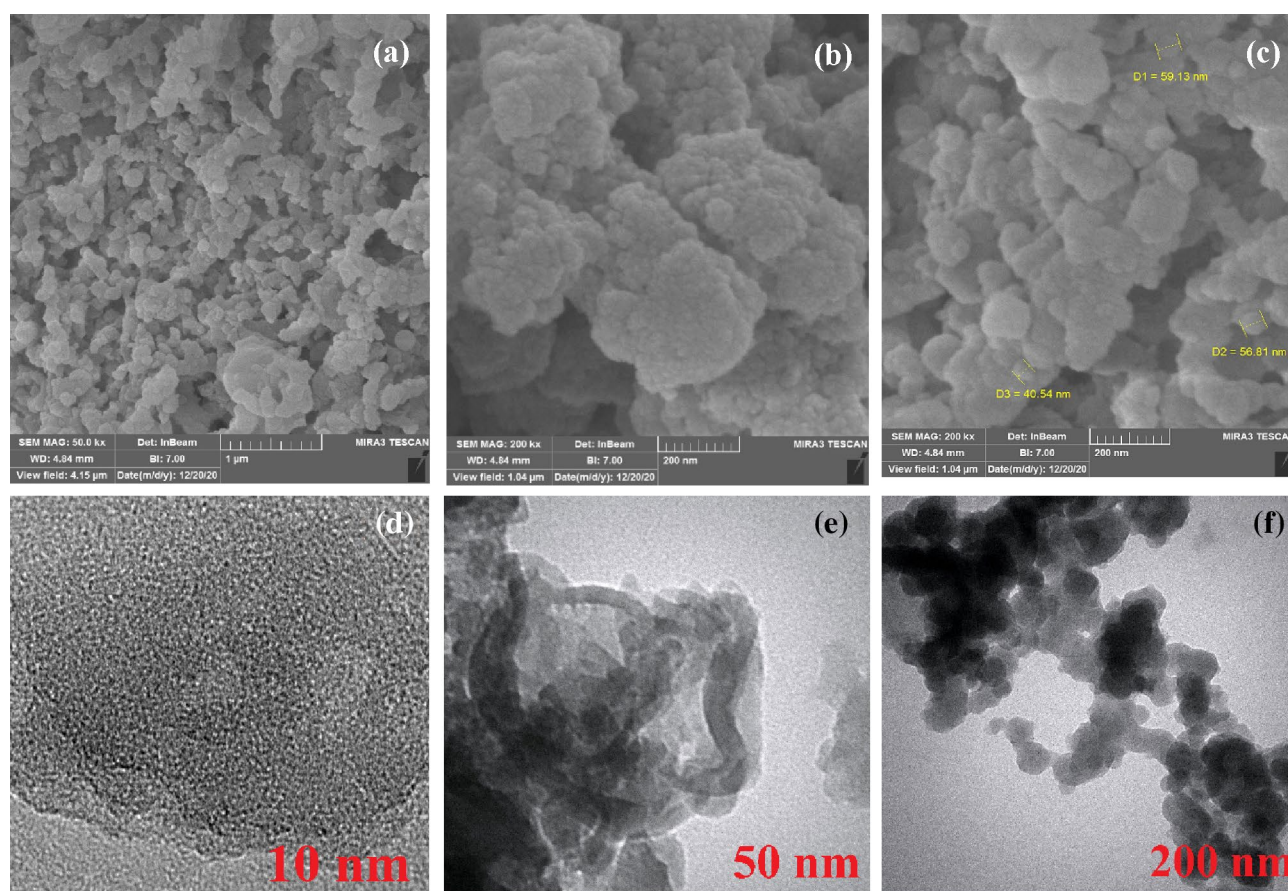


Figure 4. FESEM (a–c) and TEM images (d–f) of the Cu@APS-TDU-PMO nanoreactor (1).

There is a peak at $2\theta = 1.35^\circ$ in the low-angle XRD pattern, indicating the mesoporous structure of Cu@APS-TDU-PMO (1, Fig. 5a)¹⁵. Also, the wide-angle diffraction signal at 2θ of $20\text{--}30^\circ$, which is characteristic of mesoporous structures, is observed in the wide-angle XRD patterns of APS-TDU-PMO and Cu@APS-TDU-PMO (1, Fig. 5b,c)¹⁶. The diffraction peaks at 2θ of 44.30° , 50.30° , and 77.50° can be assigned to the reflections

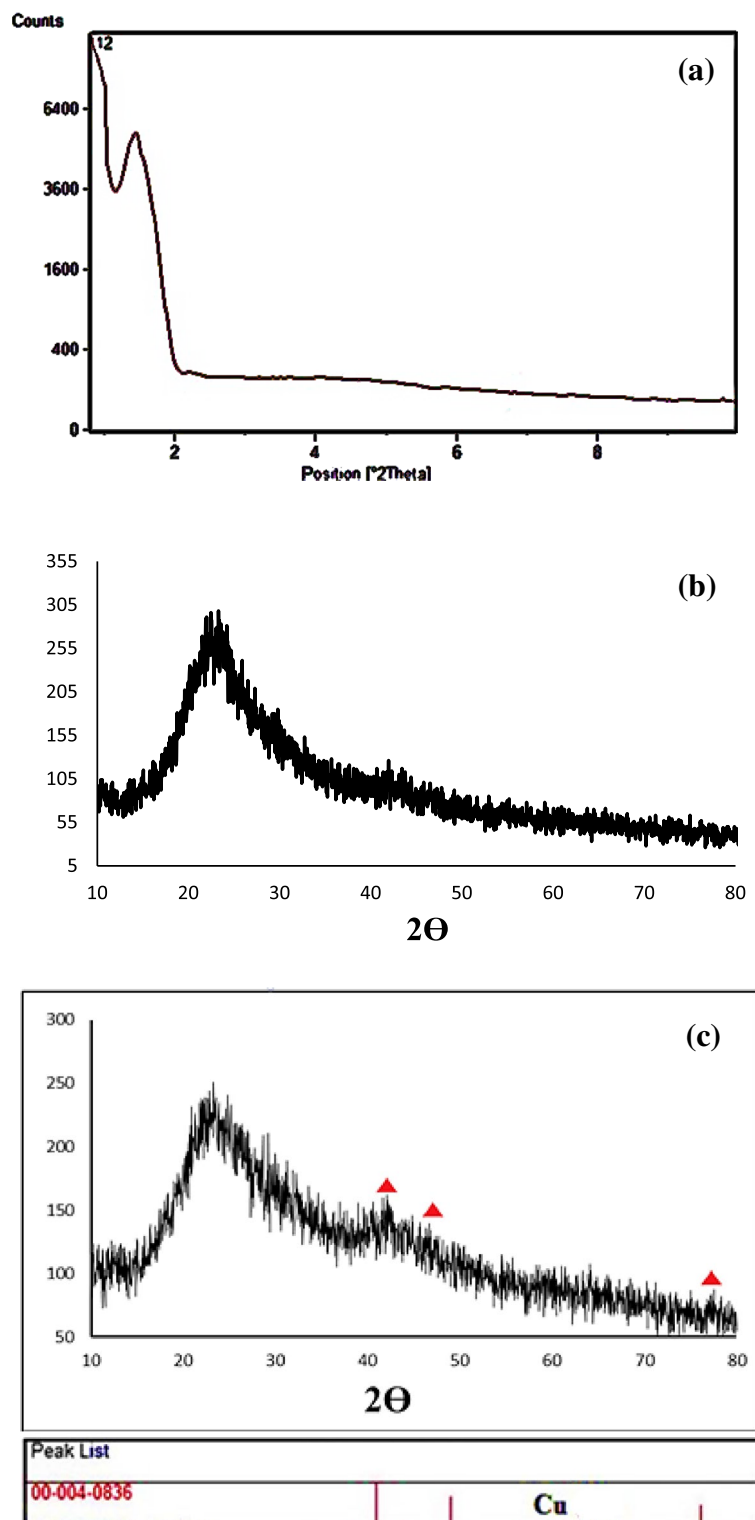


Figure 5. Low-angle (a) and wide angle (b) XRD patterns of the APS-TDU-PMO; Wide angle XRD pattern of the Cu@APS-TDU-PMO (1, c).

of Cu(II) species nanoparticles coordinated to the surface of APS-TDU-PMO¹¹⁷ (JCPDS card No. 00-004-0836, marked with ▲).

Also, EDX analysis confirmed the presence of C, N, O, Si, and Cu elements in the composition of Cu@APS-TDU-PMO (1) nanocomposite (Fig. 6).

On the other hand, the N₂ adsorption–desorption isotherm for Cu@APS-TDU-PMO nanomaterial (1) represented type IV isotherm (Fig. 7), which is commonly observed for mesoporous silica structures. The calculated

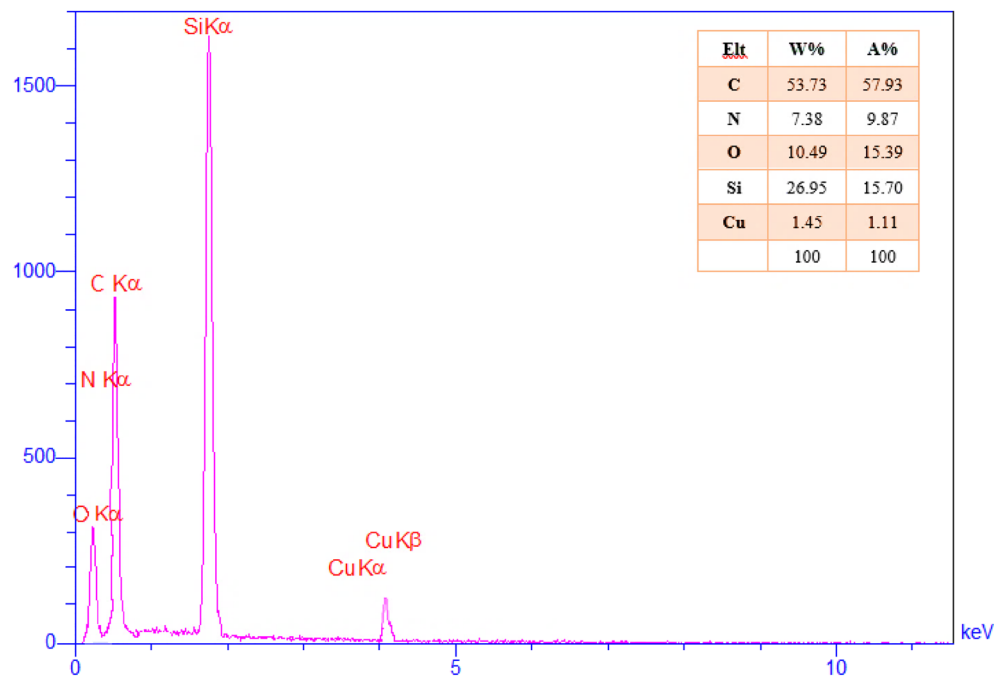


Figure 6. EDX analysis of the Cu@APS-TDU-PMO nanocomposite (1).

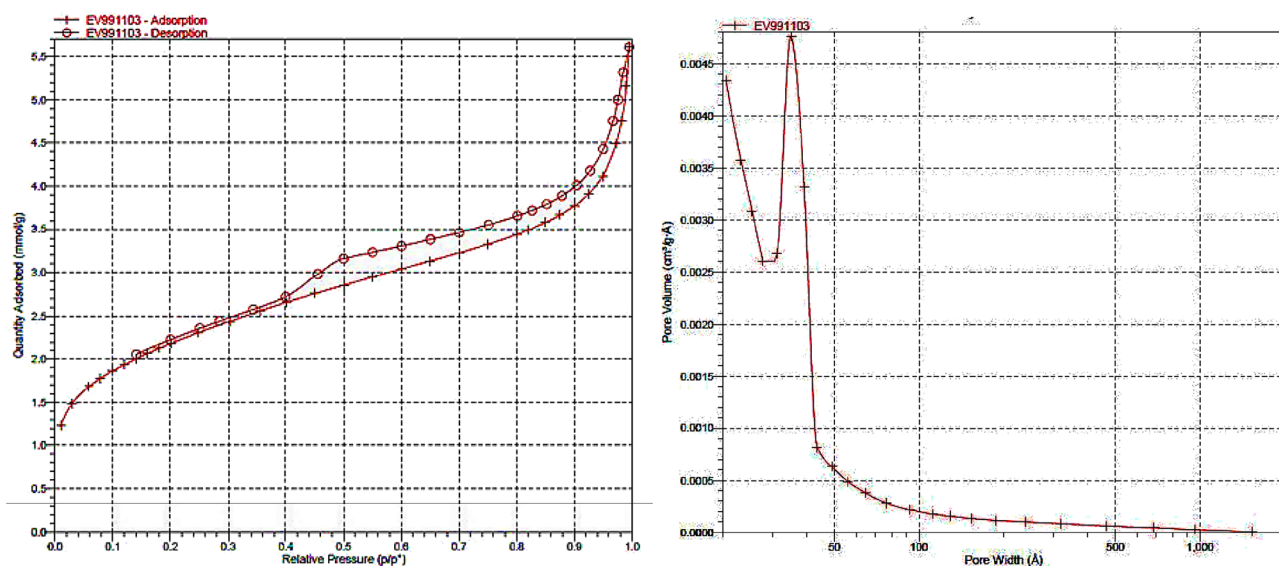


Figure 7. N₂ adsorption–desorption isotherm of the Cu@APS-TDU-PMO mesoporous material (1).

Sample	Pore diameter (nm)	Surface area (m ² g ⁻¹)	V _p (cm ³ g ⁻¹)
Cu@APS-TDU-PMO (1)	5.74	276	0.17

Table 1. Structural parameters of the Cu@APS-TDU-PMO (1) determined from N₂ adsorption–desorption experiment.

BET surface area was approximately 276 m² g⁻¹ which was retained even after the deposition of Cu(II) nanoparticles. The average pore size was about 5.74 nm (Table 1).

Catalytic application of the Cu@APS-TDU-PMO nanomaterial (1) for the synthesis of 2-(1H-tetrazol-5-yl) acrylonitrile derivatives 5a–l. The catalytic performance of the prepared Cu@

Entry	Catalyst	Catalyst loading (mg, mmol Cu(II))	Solvent	Temperature (°C)	Time (min)	Yield 5a ^a (%)	TON	TOF (h ⁻¹)
1	–	–	Solvent-free	r.t.	120	Trace	0	0
2	–	–	H ₂ O	r.t.	120	Trace	0	0
3	–	–	DMF	r.t.	120	30	0	0
4	–	–	EtOH	r.t.	120	20	0	0
5	–	–	EtOH	Reflux	120	20	0	0
6	–	–	DMF	Reflux	120	40	0	0
7	–	–	Solvent-free	110	120	45	0	0
8	APS-TDU-PMO	50	Solvent-free	110	50	30	–	–
9	Cu@APS-TDU-PMO (1)	50 (1.141 × 10 ⁻³)	EtOH	Reflux	50	38	333	400
10	Cu@APS-TDU-PMO (1)	50 (1.141 × 10 ⁻³)	DMF	Reflux	50	65	570	684
11	Cu@APS-TDU-PMO (1)	50 (1.141 × 10 ⁻³)	Solvent-free	110	50	90	789	947
12	Cu@APS-TDU-PMO (1)	50 (1.141 × 10 ⁻³)	Solvent-free	r.t.	50	Trace	–	–
13	Cu@APS-TDU-PMO (1)	50 (1.141 × 10 ⁻³)	Solvent-free	80	50	40	351	421
14	Cu@APS-TDU-PMO (1)	30 (0.685 × 10 ⁻³)	Solvent-Free	110	50	97	1416	1699
15	Cu@APS-TDU-PMO (1)	20 (0.459 × 10 ⁻³)	Solvent-free	110	50	70	1525	1830
16	Cu@APS-TDU-PMO (1)	10 (0.228 × 10 ⁻³)	Solvent-free	110	50	55	2412	2895

Table 2. Screening of optimal conditions for the synthesis of (*E*)-3-phenyl-2-(1*H*-tetrazol-5-yl)acrylonitrile product **5a**. Reaction conditions: benzaldehyde (**2a**, 1.0 mmol), malononitrile (**3**, 1.0 mmol), sodium azide (**4**, 1.2 mmol) and Cu@APS-TDU-PMO (**1**) under different conditions and solvent (2 mL, if not otherwise stated). ^aIsolated yield.

APS-TDU-PMO nanocomposite (**1**) was investigated for the synthesis of 2-(1*H*-tetrazol-5-yl) acrylonitrile derivatives in the next step of our study. To determine the optimal reaction conditions, the three-component reaction of benzaldehyde (**2a**), malononitrile (**3**) and sodium azide (**4**) was selected as the model reaction. The model reaction was investigated in different solvents at various temperatures and catalyst loadings. The optimized reaction conditions are shown in Table 2. Initially, the model reaction was performed under different conditions without any catalyst. The obtained results showed that the reaction efficiency to afford desired (*E*)-3-phenyl-2-(1*H*-tetrazol-5-yl)acrylonitrile product **5a** was negligible or low even after 120 min (Entries 1–7). Then, the model reaction was performed in EtOH and DMF as well as under solvent-free conditions in the presence of 50 mg of both APS-TDU-PMO catalysts (Entries 8–11). The model reaction was also studied at different temperatures to find 110 °C under solvent-free conditions as the optimal temperature (Entries 11–13). The results also indicated that the optimal amount of Cu@APS-TDU-PMO nanocomposite catalyst (**1**) loading is 30 mg for the model reaction. Indeed, lower amounts of catalyst loadings led to reduced efficiency of the model reaction (Entries 14–16). In order to prove the heterogeneous nature of the Cu@APS-TDU-PMO catalyst (**1**), hot filtration experiment was performed. For this purpose, the Cu@APS-TDU-PMO catalyst (**1**) was separated from the reaction mixture after 20 min. Then, the reaction continued in the absence of nanocatalyst (**1**) for another 30 min. No further increase in the conversion of benzaldehyde (**2a**) was observed, confirming presence of Cu(II) active sites for the synthesis of 2-(1*H*-tetrazol-5-yl)acrylonitrile derivative **5a** on the surface of Cu@APS-TDU-PMO nanocatalyst (**1**). Also, no effect of copper release was observed in the reaction mixture, which is well indicated by FTIR and XRD pattern analysis of the recycled catalyst **1**.

In the next step, 30 mg of the Cu@APS-TDU-PMO nanoreactor (**1**) under solvent-free conditions at 110 °C was selected as the optimal reaction conditions for the synthesis of other 2-(1*H*-tetrazol-5-yl) acrylonitrile derivatives. Various aromatic aldehydes with electron-withdrawing or electron-donating groups (entries 1–10) as well as heteroaromatic aldehydes (entries 11, 12) were involved in the optimal reaction conditions to afford the corresponding (*E*)-3-aryl/heteroyl-2-(1*H*-tetrazol-5-yl) acrylonitrile derivatives **5b–l** in high to quantitative yields. In fact, aldehydes having electron-withdrawing substitutions react more rapidly and have higher efficiencies than aldehydes containing electron-releasing groups. These observations indicate that formation of the Knoevenagel condensation intermediate may be rate-determining step of this three-component reaction. The obtained results are summarized in Table 3.

The proposed mechanism for the synthesis of 2-(1*H*-tetrazol-5-yl) acrylonitrile derivatives **5 catalysed by Cu@APS-TDU-PMO nanocatalyst (**1**).** A plausible mechanism for the synthesis of 2-(1*H*-tetrazol-5-yl) acrylonitrile derivatives in the presence of Cu@APS-TDU-PMO nanocatalyst (**1**) is shown in Fig. 8. Initially, the carbonyl group of aromatic aldehyde **2** and the nitrile group of malononitrile (**3**) are activated by the Cu@APS-TDU-PMO catalyst (**1**) to afford the Knoevenagel condensation intermediate (**I**). Then, Cu(II) species of the catalyst **1** activates one of the C≡N functional groups of the intermediate (**I**) to promote [3 + 2] cycloaddition reaction between it and sodium azide (**4**) and producing intermediate (**II**). In the next step, sodium salt of 2-(1*H*-tetrazol-5-yl) acrylonitrile derivative, as a more desirable tautomer in condensed media¹²¹, can be formed via the tautomerization of intermediate (**II**). Subsequently, the catalyst **1** is separated from the sodium salt of more stable tautomer using an aqueous solution of HCl to afford product **5**.

Comparison of the catalytic activity of Cu@APS-TDU-PMO (1**) catalyst for the synthesis of 2-(1*H*-tetrazol-5-yl) acrylonitrile derivative **5**.** To show merits of this new methodology, Table 4 compares the catalytic activity of Cu@APS-TDU-PMO (**1**) with some similar catalytic systems reported in the literature for the synthesis of (*E*)-3-phenyl-2-(1*H*-tetrazol-5-yl)acrylonitrile derivative **5a** in terms of the active catalytic sites or used support. In fact, specific advantages of Cu@APS-TDU-PMO catalyst (**1**) such as high efficiency, low catalyst loading, working under solvent-free conditions, short reaction time, and reusability make it superior to the most of similar reported protocols.

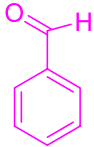
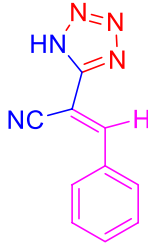
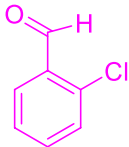
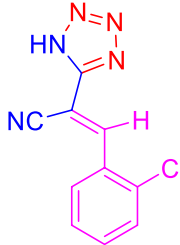
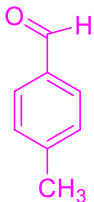
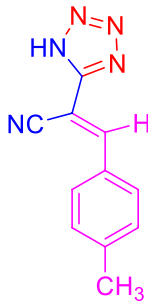
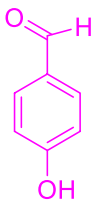
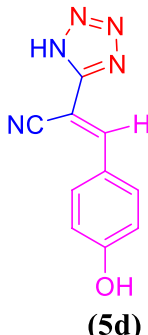
Reusability of the Cu@APS-TDU-PMO nanocatalyst (1**) for the synthesis of 2-(1*H*-tetrazol-5-yl) acrylonitrile derivative **5**.** Performing chemical reactions using recyclable and reusable catalytic systems is a significant issue in terms of green chemistry and environmental protection principles. In this study, recyclability of the Cu@APS-TDU-PMO catalyst (**1**) was also investigated. For this purpose, the catalyst was separated from the reaction mixture using filtration, then washed with EtOH, and dried at 60 °C for 2 h. The recycled catalyst **1** in each step was used in six consecutive model reaction under optimal conditions for the synthesis of (*E*)-3-phenyl-2-(1*H*-tetrazol-5-yl)acrylonitrile derivative **5a**. As shown in Fig. 9, the catalytic activity of Cu@APS-TDU-PMO (**1**) was slightly decreased from 97 to 85%. To demonstrate the stability of the Cu@APS-TDU-PMO (**1**) under optimal conditions, the FTIR spectra and low angle XRD pattern of recycled catalyst after six consecutive runs have been presented in Fig. 10.

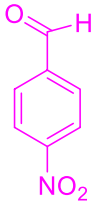
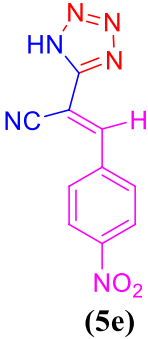
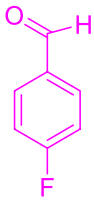
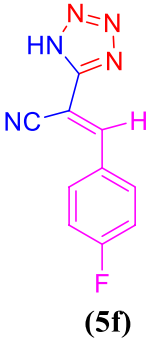
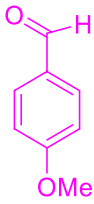
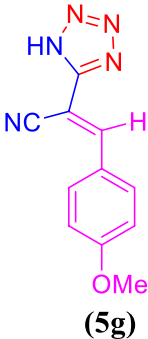
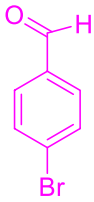
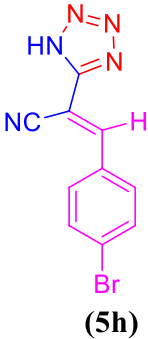
Experimental section

Materials and instrumentation. All chemicals were purchased from Merck or Aldrich and used as received, except for benzaldehyde which was distilled before its using. Characterization of the new Cu@APS-TDU-PMO (**1**) was performed by FESEM (TESCAN-MIRA3), TEM (Philips EM 208S), FTIR (Shimadzu 8400S), BET (ASAP™ 2020 Micromeritics), and TGA Bahr Company STA 504). XRD patterns of the mesoporous silica nanosphere were obtained using TW 1800 diffractometer with CuK α radiation ($\lambda = 1.54050 \text{ \AA}$). ¹H NMR and spectra (500 MHz, Bruker DRX-500 Avance spectrometer) were recorded in DMSO-*d*₆ at ambient temperature. Spectral data were compared with those obtained from authentic samples or reported in the literature. Distilled water was used in all experiments.

General procedure for the preparation of 1,3-bis(3-(triethoxysilyl)propyl) urea bridge (6**, APS-TDU).** First, (3-aminopropyl)triethoxysilane (APS, 6.16 g, 28.0 mmol) was added dropwise to toluene-2,4-diisocyanate (TDI, 2.46 g, 14.0 mmol) in a 50 mL round-bottom flask and the mixture was stirred under solvent-free condition at 75 °C for 4 h. Then, the mixture was cooled down to room temperature and stirred for 12 h to obtain a white gel. Subsequently, CHCl₃ (10 mL) was added to the white gel and a clear solution was obtained. Then, hexane (10 mL) was added to the obtained solution and a white solid was precipitated, which was separated by filtration and washed with hexane and dried at 70 °C to give 6.5 g of 1,3-bis(3-(triethoxysilyl)propyl) urea bridge (**6**, Fig. 11).

General procedure for the preparation of APS-TDU-PMO (1'**).** P123 (4.0 g), as a surfactant, was dissolved in HCl (2.0 M, 150 mL) in a 250 mL round-bottom flask and the mixture was heated to 40 °C under stirring for 4 h. Then, 1,3-bis(3-(triethoxysilyl)propyl) urea bridge (**6**, 3.5 g) was dissolved in a solution of tetraethyl orthosilicate (TEOS, 11.09 g, 53.2 mmol) in CHCl₃ (25 mL). The obtained solution was added dropwise to the solution of P123 and HCl and stirred for 24 h at 40 °C and then aging for 48 h at 100 °C. Eventually, the obtained white solid was washed with EtOH (10 mL) and hexane (10 mL) and dried at 80 °C. The surfactant was extracted under Soxhlet extraction conditions using EtOH-aqueous HCl for 72 h. Finally, the white solid was dried at 100 °C for 12 h to give 6.0 g of APS-TDU-PMO (**1'**, Fig. 11).

Entry	Substrate (2)	Product	Time (min)	Yield (%)	Mp (°C)	
					Observed	Reference
1	 (2a)	 (5a)	50	97	168–169	170–171 ¹¹⁸
2	 (2b)	 (5b)	52	93	174–176	175–177 ¹¹⁹
3	 (2c)	 (5c)	55	92	189–191	189–191 ¹¹⁸
4	 (2d)	 (5d)	60	89	158–160	159–161 ¹¹⁸
Continued						

Entry	Substrate (2)	Product	Time (min)	Yield (%)	Mp (°C)	
					Observed	Reference
5	 <p>(2e)</p>	 <p>(5e)</p>	60	91	167–168	166–168 ¹²⁰
6	 <p>(2f)</p>	 <p>(5f)</p>	56	93	177–179	176–179 ¹¹⁹
7	 <p>(2g)</p>	 <p>(5g)</p>	53	92	152–153	153–155 ¹¹⁸
8	 <p>(2h)</p>	 <p>(5h)</p>	56	89	164–166	165–167 ¹²⁰
Continued						

Entry	Substrate (2)	Product	Time (min)	Yield (%)	Mp (°C)	
					Observed	Reference
9	(2i)	(5i)	52	92	143–145	142–143 ¹²⁰
10	(2j)	(5j)	40	95	166–168	165–168 ¹¹⁸
11	(2k)	(5k)	56	90	87–88	85–86 ¹²⁰
12	(2l)	(5l)	55	93	252–254	253–254 ¹²⁰

Table 3. Scope of the synthesis of different 2-(1H-tetrazol-5-yl) acrylonitrile derivatives **5a–l** catalysed by Cu@APS-TDU-PMO nanoreactor (**1**). Reaction conditions: aldehydes (**2**, 1 mmol), malononitrile (**3**, 1 mmol), sodium azide (**4**, 1.2 mmol) and Cu@APS-TDU-PMO (**1**, 0.03 g) under solvent-free conditions conditions.

General procedure for the preparation of Cu@APS-TDU-PMO (1). Cu(OAc)₂ (0.5 g, 2.8 mmol) was dissolved in 5.0 mL distilled water and the obtained solution was added slowly to the suspension of APS-TDU-PMO (0.5 g) in distilled water (10 mL). The obtained mixture was stirred at room temperature for 24 h. Finally, the resulting green solid was collected, washed with distilled water and EtOH, and then dried at 60 °C for 5 h to afford Cu@APS-TDU-PMO (**1**, 0.7 g, Fig. 11).

General procedure for the preparation of 2-(1H-tetrazol-5-yl) acrylonitrile derivatives 5a–l. Cu@APS-TDU-PMO (**1**, 30 mg), aromatic aldehyde (**2a–l**, 1.0 mmol), malononitrile (**3**, 1.0 mmol), and NaN₃ (**4**, 1.20 mmol) were mixed, in a 10 mL round-bottom flask equipped with a magnetic stirrer and con-

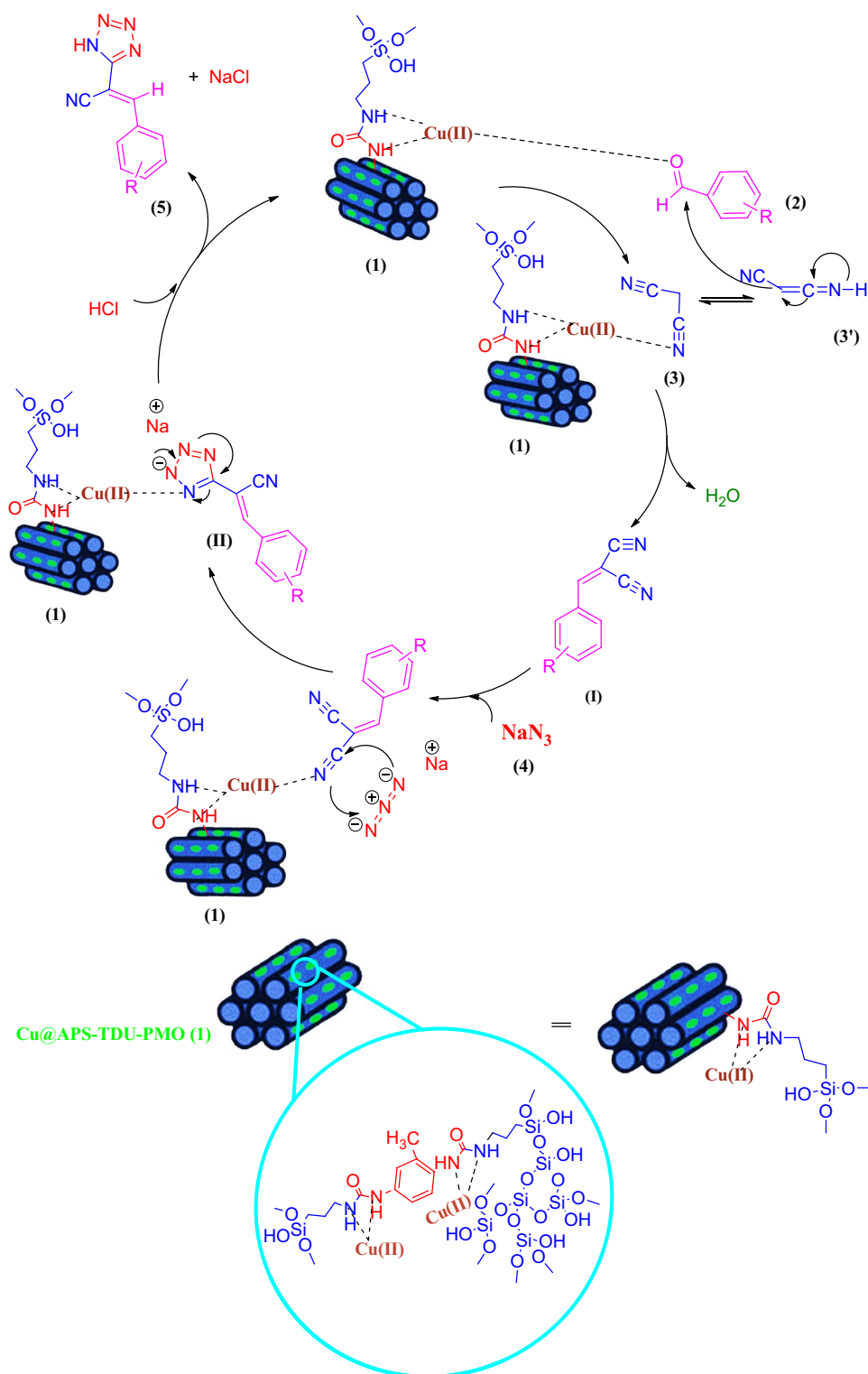


Figure 8. The proposed mechanism for the synthesis of 2-(1H-tetrazol-5-yl) acrylonitrile derivatives in the presence of Cu@APS-TDU-PMO nanoreactor (1).

denser, and then heated under solvent-free conditions to 110 °C. The reaction progress was monitored by TLC. After completion of the reaction, the reaction mixture was dispersed in HCl (2.0 M, 2 mL) and EtOAc (10 mL) was added and stirred for 15 min. Then, the solid catalyst **1** was separated by filtration and filtrate was extracted using EtOAc (5 mL). Finally, the solvent of collected organic layers was evaporated under reduced pressure on a rotary evaporator and the obtained solids were recrystallized in EtOH/H₂O to afford the pure products **5a–l**. The recovered catalyst was reused after drying at 100 °C for 2 h for subsequent cycles.

Entry	Catalyst	Catalyst loading (mg)	Temperature (°C)	Time (min)	References
1	Nano-NiO	4.5	70	360	¹²²
2	Fe ₃ O ₄ @APTMS-DFX	30	120	60	¹²³
3	Cu-MCM-41	30	140	720	¹²⁴
4	Mesoporous ZnS	91	120	36 h	¹²⁵
5	Cu@APS-TDU-PMO (1)	30	110	30	This work

Table 4. Comparison of the catalytic activity of Cu@APS-TDU-PMO (1) with other reported catalytic systems.

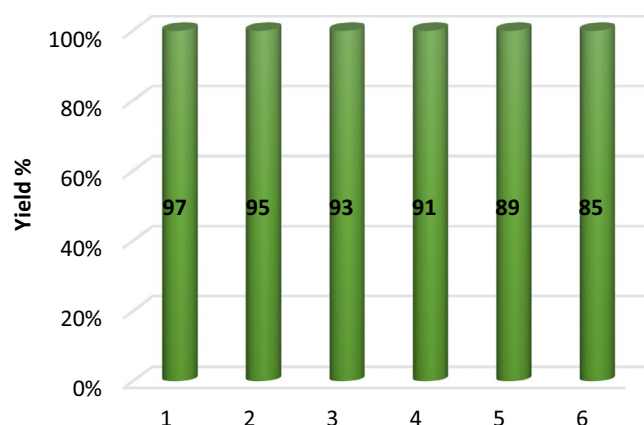


Figure 9. Reusability of the heterogeneous Cu@APS-TDU-PMO catalyst (1) for the synthesis of 5a.

The FTIR, ¹H NMR and ¹³C NMR data of selected tetrazole derivatives. (*E*)-3-(2-Chlorophenyl)-2-(1*H*-tetrazole-5-yl)acrylonitrile (**5b**). FTIR (KBr disc): $\bar{\nu}$ (cm⁻¹), 3420 (NH), 2221 (C≡N), 1564 (C=C); ¹H NMR (500 MHz, DMSO-*d*₆): δ (ppm), 7.58–7.59 (2H, d, CH-Ar), 7.61–7.69 (1H, t, *J* = 7.2 Hz, CH-Ar), 8.13–8.14 (1H, d, CH-Ar), 8.54 (1H, s, CH), 13.22 (br s, NH); ¹³C NMR (125 MHz, DMSO-*d*₆): δ (ppm), 80.14, 116.80, 129.17, 129.88, 130.73, 131.97, 134.39, 135.19, 147.04, 159.07, 161.37.

(*E*)-3-(4-Methoxyphenyl)-2-(1*H*-tetrazole-5-yl)acrylonitrile (**5g**). FTIR (KBr, disc): $\bar{\nu}$ (cm⁻¹), 3146 (NH), 2224 (C≡N), 1586 (C=C); ¹H NMR (500 MHz, DMSO-*d*₆): δ (ppm), 3.82 (3H, s, OCH₃), 7.09–7.11 (1H, d, CH-Ar), 7.96–7.99 (1H, d, CH-Ar), 8.21 (1H, s, CH), 13.70 (br s, NH); ¹³C NMR (125 MHz, DMSO-*d*₆): δ (ppm), 56.02, 93.70, 115.25, 116.55, 125.21, 132.61, 147.97, 155.85, 162.91.

Conclusions

In conclusion, the supramolecular toluene-2,4-diurea-based periodic mesoporous organosilica containing Cu nanoparticles on its pore wall (Cu@APS-TDU-PMO) was synthesized for the first time. The prepared Cu@APS-TDU-PMO (1) was characterized by using FTIR, EDX, TGA, XRD, FESEM, BET, and TEM spectroscopic, microscopic or analytical methods and techniques. The Cu@APS-TDU-PMO showed unique characteristics such as porous structure with adjustable and uniform pore size distribution, high thermal stability and surface area. The new Cu@APS-TDU-PMO nanomaterial was efficiently used as a promising and recyclable catalyst for the synthesis of different 2-(1*H*-tetrazol-5-yl)acrylonitrile derivatives through multicomponent strategy under solvent-free conditions. In addition, the catalyst can be easily separated by filtration and reused several times without significant loss of its catalytic activity.

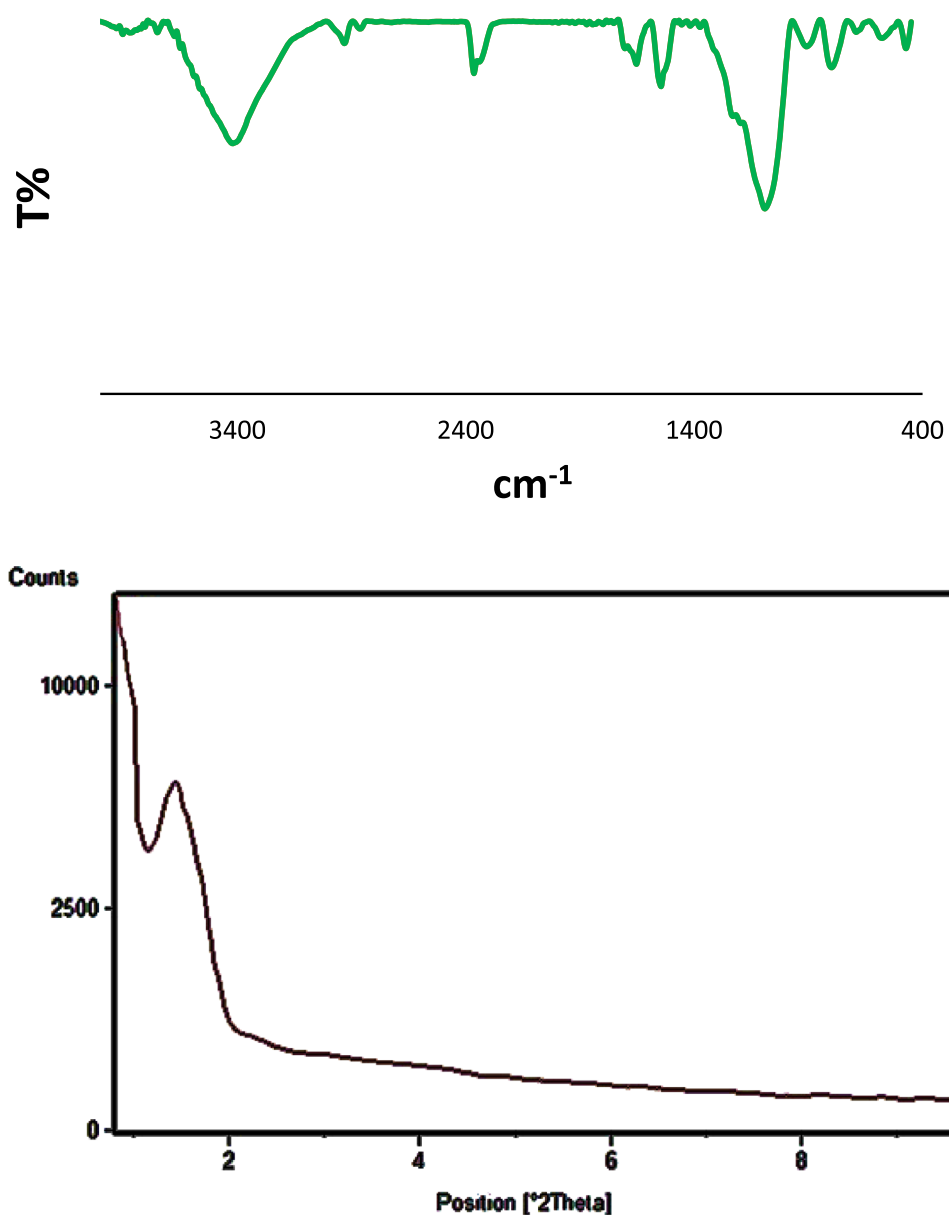


Figure 10. FTIR spectra and low angle XRD pattern of the reused Cu@APS-TDU-PMO catalyst (1) after six consecutive runs.

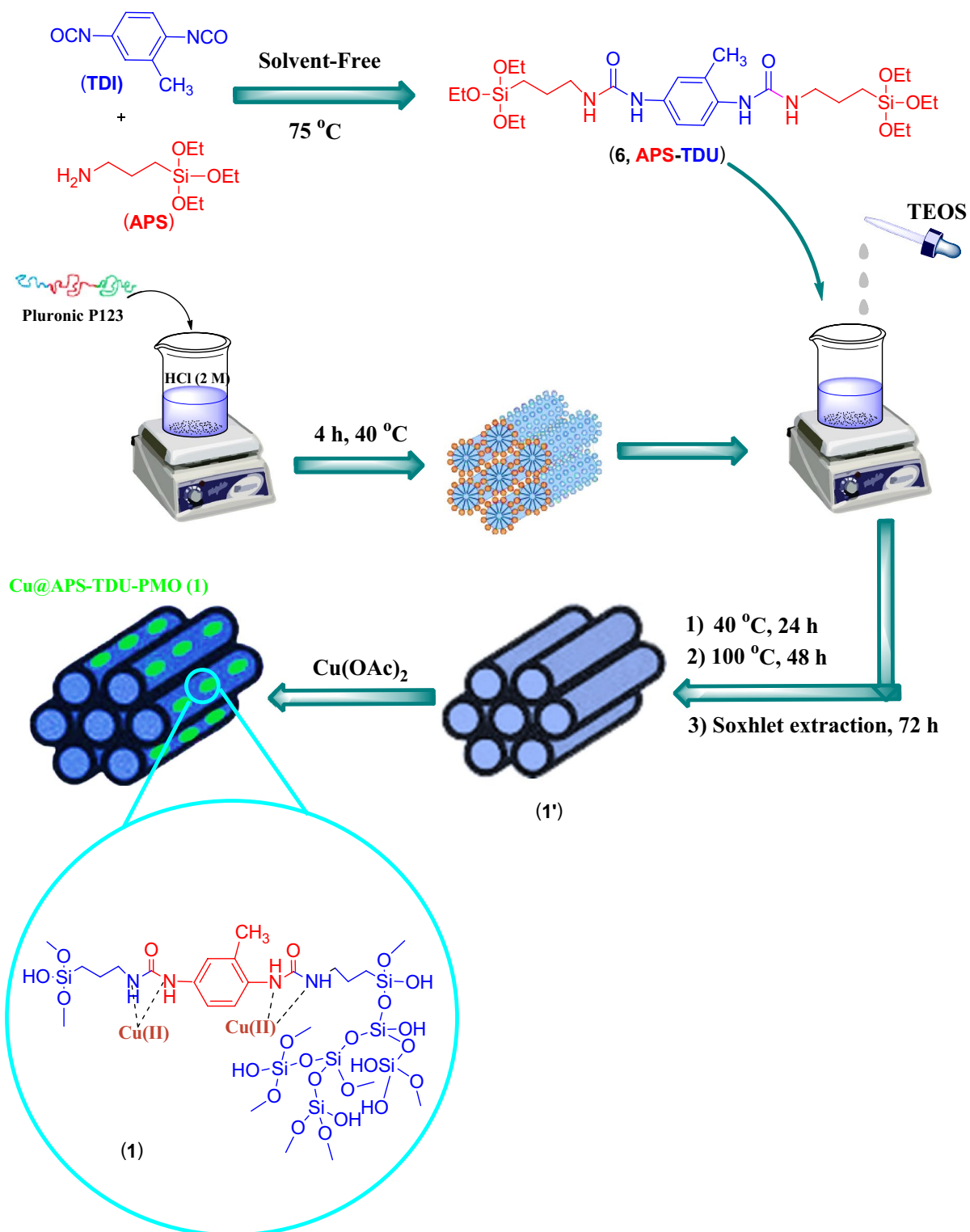


Figure 11. General procedure for the preparation of Cu@APS-TDU-PMO nanocatalyst (1).

Data availability

All data generated or analyzed during this study are included in this published article [and its supplementary information files].

Received: 6 April 2022; Accepted: 20 October 2022

Published online: 28 October 2022

References

- Corma, A. From microporous to mesoporous molecular sieve materials and their use in catalysis. *Chem. Rev.* **97**, 2373–2420 (1997).
- Sayari, A. & Hamoudi, S. Periodic mesoporous silica-based organic–inorganic nanocomposite materials. *Chem. Mater.* **13**, 3151–3168 (2001).
- Ying, J. Y., Mehnert, C. P. & Wong, M. S. Synthesis and applications of supramolecular-templated mesoporous materials. *Angew. Chem. Int. Ed.* **38**, 56–77 (1999).
- Liu, X., Li, J., Zhou, L., Huang, D. & Zhou, Y. Adsorption of CO₂, CH₄ and N₂ on ordered mesoporous silica molecular sieve. *Chem. Phys. Lett.* **415**, 198–201 (2005).
- Grün, M., Kurganov, A., Schacht, S., Schüth, F. & Unger, K. Comparison of an ordered mesoporous aluminosilicate, silica, alumina, titania and zirconia in normal-phase high-performance liquid chromatography. *J. Chromatogr. A* **740**, 1–9 (1996).
- Raja, R. & Thomas, J. M. Catalyst design strategies for controlling reactions in microporous and mesoporous molecular-sieves. *J. Mol. Catal. A: Chem.* **181**, 3–14 (2002).
- Jalili, F., Zarei, M., Zolfigol, M. A., Rostamnia, S. & Moosavi-Zare, A. R. SBA-15/PrN (CH₂PO₃H₂)₂ as a novel and efficient mesoporous solid acid catalyst with phosphorous acid tags and its application on the synthesis of new pyrimido [4,5-b] quinolones and pyrido [2,3-d] pyrimidines via anomeric based oxidation. *Microporous Mesoporous Mater.* **294**, 109865 (2020).
- Shaker, M. & Elhamifar, D. Magnetic methylene-based mesoporous organosilica composite-supported IL/Pd: A powerful and highly recoverable catalyst for oxidative coupling of phenols and naphthols. *Mater. Today Chem.* **18**, 100377 (2020).
- dos Santos Andrade, L., Otubo, L., Castanheira, B. & Brochsztain, S. Novel periodic mesoporous organosilicas containing pyromellitimides and their application for the photodegradation of asphaltenes. *Microporous Mesoporous Mater.* **312**, 110740 (2021).
- Zhao, W. *et al.* Light-responsive dual-functional biodegradable mesoporous silica nanoparticles with drug delivery and lubrication enhancement for the treatment of osteoarthritis. *Nanoscale* **13**, 6394–6399 (2021).
- Liu, W. *et al.* Rational design of lanthanide nano periodic mesoporous organosilicas (Ln-nano-PMOs) for near-infrared emission. *Dalton Trans.* **50**, 2774–2781 (2021).
- Castillo, X. *et al.* A cheap mesoporous silica from fly ash as an outstanding adsorbent for sulfate in water. *Microporous Mesoporous Mater.* **272**, 184–192 (2018).
- Zhang, Z., Huang, Z. & Yuan, H. Direct conversion of cellulose to ethyl levulinate catalysed by modified fibrous mesoporous silica nanospheres in a co-solvent system. *New J. Chem.* **45**, 5526–5539 (2021).
- El-Sewify, I. M. & Khalil, M. M. Mesoporous nanosensors for sensitive monitoring and removal of copper ions in wastewater samples. *New J. Chem.* **45**, 2573–2581 (2021).
- Chatterjee, S. *et al.* Catalytic transformation of ethanol to methane and butene over NiO NPs supported over mesoporous SBA-15. *Mol. Catal.* **502**, 111381 (2021).
- Nikooei, N., Dekamin, M. G. & Valiey, E. Benzene-1,3,5-tricarboxylic acid-functionalized MCM-41 as a novel and recoverable hybrid catalyst for expeditious and efficient synthesis of 2,3-dihydroquinazolin-4(1H)-ones via one-pot three-component reaction. *Res. Chem. Intermed.* **46**, 3891–3909. <https://doi.org/10.1007/s11164-020-04179-8> (2020).
- Shendabadi, A. R. *et al.* 1,3,5-Tris (2-hydroxyethyl) isocyanurate functionalized SBA-15 (THEIC-SBA-15): As a novel heterogeneous nano-catalyst for the one-pot three-component synthesis of tetrahydrobenzo b pyrans in water. *Biointerface Res. Appl. Chem.* **10**, 6706–6717. <https://doi.org/10.33263/BRIAC106.67066717> (2020).
- Sam, M., Dekamin, M. G. & Alirezvani, Z. Dendrons containing boric acid and 1,3,5-tris(2-hydroxyethyl)isocyanurate covalently attached to silica-coated magnetite for the expeditious synthesis of Hantzsch esters. *Sci. Rep.* **11**, 2399. <https://doi.org/10.1038/s41598-020-80884-z> (2021).
- Cao, L. *et al.* Fluorophore-free luminescent double-shelled hollow mesoporous silica nanoparticles as pesticide delivery vehicles. *Nanoscale* **10**, 20354–20365 (2018).
- Olivieri, F., Castaldo, R., Cocca, M., Gentile, G. & Lavorgna, M. Mesoporous silica nanoparticles as carriers of active agents for smart anticorrosive organic coatings: A critical review. *Nanoscale* **13**, 9091–9111 (2021).
- Zebardasti, A., Dekamin, M. G., Doustkhah, E. & Assadi, M. H. N. Carbamate-isocyanurate-bridged periodic mesoporous organosilica for van der Waals CO₂ capture. *Inorg. Chem.* **59**, 11223–11227. <https://doi.org/10.1021/acs.inorgchem.0c01449> (2020).
- Zebardasti, A., Dekamin, M. G. & Doustkhah, E. The isocyanurate-carbamate-bridged hybrid mesoporous organosilica: An exceptional anchor for Pd nanoparticles and a unique catalyst for nitroaromatics reduction. *Catalysts* **11**, 621. <https://doi.org/10.3390/catal11050621> (2021).
- Kumar, S., Malik, M. & Purohit, R. Synthesis methods of mesoporous silica materials. *Mater. Today Proc.* **4**, 350–357 (2017).
- Amiri, A. A., Javanshir, S., Dolatkah, Z. & Dekamin, M. G. SO₃H-functionalized mesoporous silica materials as solid acid catalyst for facile and solvent-free synthesis of 2H-indazolo [2,1-b] phthalazine-1,6,11-trione derivatives. *New J. Chem.* **39**, 9665–9671. <https://doi.org/10.1039/C5NJ01733E> (2015).
- Cao, M. *et al.* New bi-functionalized ordered mesoporous material as heterogeneous catalyst for production of 5-hydroxymethylfurfural. *Microporous Mesoporous Mater.* **312**, 110709 (2021).
- Valiey, E., Dekamin, M. G. & Alirezvani, Z. Sulfamic acid pyromellitic diamide-functionalized MCM-41 as a multifunctional hybrid catalyst for melting-assisted solvent-free synthesis of bioactive 3,4-dihydropyrimidin-2-(1H)-ones. *Sci. Rep.* **11**, 11199. <https://doi.org/10.1038/s41598-021-89572-y> (2021).
- Wei, Y. *et al.* Periodic mesoporous organosilica nanocubes with ultrahigh surface areas for efficient CO₂ adsorption. *Sci. Rep.* **6**, 1–11 (2016).
- Matsukawa, H. *et al.* Fast and stable vapochromic response induced through nanocrystal formation of a luminescent platinum (II) complex on periodic mesoporous organosilica. *Sci. Rep.* **9**, 1–11 (2019).
- Mohanty, P. & Landskron, K. Periodic mesoporous organosilica nanorice. *Nanoscale Res. Lett.* **4**, 169. <https://doi.org/10.1007/s11671-008-9219-0> (2008).
- Akbari, A., Dekamin, M. G., Yaghoubi, A. & Naimi-Jamal, M. R. Novel magnetic propylsulfonic acid-anchored isocyanurate-based periodic mesoporous organosilica (iron oxide@PMO-ICS-PrSO₃H) as a highly efficient and reusable nanoreactor for the sustainable synthesis of imidazopyrimidine derivatives. *Sci. Rep.* **10**, 10646. <https://doi.org/10.1038/s41598-020-67592-4> (2020).
- Van Der Voort, P. *et al.* Periodic mesoporous organosilicas: from simple to complex bridges; a comprehensive overview of functions, morphologies and applications. *Chem. Soc. Rev.* **42**, 3913–3955 (2013).
- Rajabi, F., Karimi, N., Luque, R. & Voskressensky, L. Highly ordered mesoporous functionalized pyridinium protic ionic liquid framework as a highly efficient catalytic system in chemoselective thioacetalization of carbonyl compounds under solvent-free conditions. *Mol. Catal.* **515**, 111919 (2021).
- Yaghoubi, A. & Dekamin, M. G. Green and facile synthesis of 4H-pyran scaffold catalyzed by pure nano-ordered periodic mesoporous organosilica with isocyanurate framework (PMO-ICS). *ChemistrySelect* **2**, 9236–9243. <https://doi.org/10.1002/slct.201700717> (2017).

34. Yaghoubi, A., Dekamin, M. G. & Karimi, B. Propylsulfonic acid-anchored isocyanurate-based periodic mesoporous organosilica (PMO-ICS-PrSO₃H): A highly efficient and recoverable nanopororous catalyst for the one-pot synthesis of substituted polyhydroquinolines. *Catal. Lett.* **147**, 2656–2663. <https://doi.org/10.1007/s10562-017-2159-5> (2017).
35. Yaghoubi, A., Dekamin, M. G., Arefi, E. & Karimi, B. Propylsulfonic acid-anchored isocyanurate-based periodic mesoporous organosilica (PMO-ICS-Pr-SO₃H): A new and highly efficient recoverable nanopororous catalyst for the one-pot synthesis of bis(indolyl) methane derivatives. *J. Colloid Interface Sci.* **505**, 956–963. <https://doi.org/10.1016/j.jcis.2017.06.055> (2017).
36. Elhamifar, D., Nasr-Esfahani, M., Karimi, B., Moshkelgosh, R. & Shabani, A. Ionic liquid and sulfonic acid based bifunctional periodic mesoporous organosilica (BPMO-IL-SO₃H) as a highly efficient and reusable nanocatalyst for the biginelli reaction. *ChemCatChem* **6**, 2593–2599 (2014).
37. Kaczmarek, A. M. *et al.* Amine-containing (nano-)periodic mesoporous organosilica and its application in catalysis, sorption and luminescence. *Microporous Mesoporous Mater.* **291**, 109687 (2020).
38. Dekamin, M. G., Arefi, E. & Yaghoubi, A. Isocyanurate-based periodic mesoporous organosilica (PMO-ICS): A highly efficient and recoverable nanocatalyst for the one-pot synthesis of substituted imidazoles and benzimidazoles. *RSC Adv.* **6**, 86982–86988. <https://doi.org/10.1039/C6RA14550G> (2016).
39. Li, P. *et al.* Selective oxidation of benzylic C–H bonds catalyzed by Cu (II)/{Pmo12}. *J. Org. Chem.* **85**, 3101–3109 (2020).
40. Lin, X.-T. *et al.* Immobilized Zn (OAc)₂ on bipyridine-based periodic mesoporous organosilica for N-formylation of amines with CO₂ and hydrosilanes. *New J. Chem.* **45**, 9501–9505 (2021).
41. Doustkhah, E. *et al.* Merging periodic mesoporous organosilica (PMO) with mesoporous aluminosilica (Al/Si-PMO): A catalyst for green oxidation. *Mol. Catal.* **482**, 110676 (2020).
42. Asefa, T., MacLachlan, M. J., Coombs, N. & Ozin, G. A. Periodic mesoporous organosilicas with organic groups inside the channel walls. *Nature* **402**, 867–871 (1999).
43. Inagaki, S., Guan, S., Fukushima, Y., Ohsuna, T. & Terasaki, O. Novel mesoporous materials with a uniform distribution of organic groups and inorganic oxide in their frameworks. *J. Am. Chem. Soc.* **121**, 9611–9614 (1999).
44. Karimi, B., Ganji, N., Pourshiani, O. & Thiel, W. R. Periodic mesoporous organosilicas (PMOs): From synthesis strategies to applications. *Prog. Mater. Sci.* **125**, 100896. <https://doi.org/10.1016/j.pmatsci.2021.100896> (2022).
45. Alirezvani, Z., Dekamin, M. G. & Valiey, E. New hydrogen-bond-enriched 1,3,5-tris(2-hydroxyethyl) isocyanurate covalently functionalized MCM-41: An efficient and recoverable hybrid catalyst for convenient synthesis of acridinedione derivatives. *ACS Omega* **4**, 20618–20633. <https://doi.org/10.1021/acsomega.9b02755> (2019).
46. Eslami, M., Dekamin, M. G., Motlagh, L. & Maleki, A. MCM-41 mesoporous silica: A highly efficient and recoverable catalyst for rapid synthesis of α -aminonitriles and imines. *Green Chem. Lett. Rev.* **11**, 36–46. <https://doi.org/10.1080/17518253.2017.1421269> (2018).
47. Kresge, C. T., Leonowicz, M. E., Roth, W. J., Vartuli, J. C. & Beck, J. S. Ordered mesoporous molecular sieves synthesized by a liquid-crystal template mechanism. *Nature* **359**, 710–712 (1992).
48. Zhao, D. *et al.* Triblock copolymer syntheses of mesoporous silica with periodic 50 to 300 angstrom pores. *Science* **279**, 548–552 (1998).
49. Mashayekhi, S. *et al.* Curcumin-loaded mesoporous silica nanoparticles/nanofiber composites for supporting long-term proliferation and stemness preservation of adipose-derived stem cells. *Int. J. Pharm.* **587**, 119656 (2020).
50. Teng, Z. *et al.* Facile synthesis of yolk-shell-structured triple-hybridized periodic mesoporous organosilica nanoparticles for biomedicine. *Small* **12**, 3550–3558 (2016).
51. Sim, K. *et al.* CO₂ adsorption on amine-functionalized periodic mesoporous benzenesilicas. *ACS Appl. Mater. Interfaces.* **7**, 6792–6802 (2015).
52. De Canck, E., Ascoop, I., Sayari, A. & Van Der Voort, P. Periodic mesoporous organosilicas functionalized with a wide variety of amines for CO₂ adsorption. *Phys. Chem. Chem. Phys.* **15**, 9792–9799 (2013).
53. De Canck, E., Esquivel, D., Romero-Salguero, F. J. & Van Der Voort, P. Periodic mesoporous organosilicas: Hybrid porous materials with exciting applications. *Compr. Guide Mesoporous Mater.* **197** (2015).
54. Kaczmarek, A. M. & Van Der Voort, P. Light-emitting lanthanide periodic mesoporous organosilica (PMO) hybrid materials. *Materials* **13**, 566 (2020).
55. Wu, C. *et al.* Clickable periodic mesoporous organosilica monolith for highly efficient capillary chromatographic separation. *Anal. Chem.* **88**, 1521–1525 (2016).
56. Ha, C.-S. & Park, S. S. *Periodic Mesoporous Organosilicas: Preparation, Properties and Applications* (eds Ha, C.-S. & Park, S. S.) 125–187 (Springer Singapore, 2019).
57. Liu, J. *et al.* Yolk-shell hybrid materials with a periodic mesoporous organosilica shell: Ideal nanoreactors for selective alcohol oxidation. *Adv. Funct. Mater.* **22**, 591–599 (2012).
58. Liu, X., Maegawa, Y., Goto, Y., Hara, K. & Inagaki, S. Heterogeneous catalysis for water oxidation by an iridium complex immobilized on bipyridine-periodic mesoporous organosilica. *Angew. Chem. Int. Ed.* **55**, 7943–7947 (2016).
59. Valiey, E. & Dekamin, M. G. Pyromellitic diamide-diacid bridged mesoporous organosilica nanospheres with controllable morphologies: A novel PMO for the facile and expeditious synthesis of imidazole derivatives. *Nanoscale Adv.* **4**, 294–308. <https://doi.org/10.1039/D1NA00738F> (2022).
60. Valiey, E. & Dekamin, M. G. Supported copper on a diamide-diacid-bridged PMO: An efficient hybrid catalyst for the cascade oxidation of benzyl alcohols/Knoevenagel condensation. *RSC Adv.* **12**, 437–450. <https://doi.org/10.1039/D1RA06509B> (2022).
61. Bryan, M. C. *et al.* Key Green Chemistry research areas from a pharmaceutical manufacturers' perspective revisited. *Green Chem.* **20**, 5082–5103. <https://doi.org/10.1039/C8GC01276H> (2018).
62. Jing, Y., Guo, Y., Xia, Q., Liu, X. & Wang, Y. Catalytic production of value-added chemicals and liquid fuels from lignocellulosic biomass. *Chem* **5**, 2520–2546. <https://doi.org/10.1016/j.chempr.2019.05.022> (2019).
63. Armor, J. N. A history of industrial catalysis. *Catal. Today* **163**, 3–9. <https://doi.org/10.1016/j.cattod.2009.11.019> (2011).
64. Nope, E. *et al.* Solvent-free microwave-assisted multicomponent synthesis of 4H-chromenes using Fe₃O₄-based hydrotalcites as bifunctional catalysts. *ChemistrySelect* **7**, e202104360 (2022).
65. Sonawane, H. R., Deore, J. V. & Chavan, P. N. Reusable nano catalysed synthesis of heterocycles: An overview. *ChemistrySelect* **7**, e202103900 (2022).
66. Dong, L. N., Wang, Y. M., Zhang, W. L., Mo, L. P. & Zhang, Z. H. Nickel supported on magnetic biochar as a highly efficient and recyclable heterogeneous catalyst for the one-pot synthesis of spirooxindole-dihydropyridines. *Appl. Organomet. Chem.* **36**, e6667 (2022).
67. Mirhosseini-Eshkevari, B., Ghasemzadeh, M. A. & Safaei-Ghomi, J. An efficient and green one-pot synthesis of indazole [1,2-b]-phthalazinetriones via three-component reaction of aldehydes, dimedone, and phthalhydrazide using Fe₃O₄@SiO₂ core-shell nanoparticles. *Res. Chem. Intermed.* **41**, 7703–7714 (2015).
68. Mohammadi, M., Khodamorady, M., Tahmasbi, B., Bahrami, K. & Ghorbani-Choghamarani, A. Boehmite nanoparticles as versatile support for organic-inorganic hybrid materials: Synthesis, functionalization, and applications in eco-friendly catalysis. *J. Ind. Eng. Chem.* **97**, 1–78 (2021).
69. Baig, N., Kammakam, I. & Falath, W. Nanomaterials: A review of synthesis methods, properties, recent progress, and challenges. *Mater. Adv.* **2**, 1821–1871. <https://doi.org/10.1039/D0MA00807A> (2021).

70. Kazemi, M. & Mohammadi, M. Magnetically recoverable catalysts: Catalysis in synthesis of polyhydroquinolines. *Appl. Organomet. Chem.* **34**, e5400 (2020).
71. Ramish, S. M., Ghorbani-Choghamarani, A. & Mohammadi, M. Microporous hierarchically Zn-MOF as an efficient catalyst for the Hantzsch synthesis of polyhydroquinolines. *Sci. Rep.* **12**, 1–15 (2022).
72. Ghasemzadeh, M. A. & Azimi-Nasrabad, M. Nano-Fe₃O₄-encapsulated silica particles bearing sulfonic acid groups as a magnetically separable catalyst for the green and efficient synthesis of 14-aryl-14H-dibenzo [a, i] xanthene-8, 13-dione derivatives. *Res. Chem. Intermed.* **42**, 1057–1069 (2016).
73. Daraie, M., Tamoradi, T., Heravi, M. M. & Karmakar, B. Ce immobilized 1H-pyrazole-3, 5-dicarboxylic acid (PDA) modified CoFe₂O₄: A potential magnetic nanocomposite catalyst towards the synthesis of diverse benzo [a] pyrano [2, 3-c] phenazine derivatives. *J. Mol. Struct.* **1245**, 131089 (2021).
74. Gawande, M. B. *et al.* Cu and Cu-based nanoparticles: Synthesis and applications in catalysis. *Chem. Rev.* **116**, 3722–3811. <https://doi.org/10.1021/acs.chemrev.5b00482> (2016).
75. Tamilvanan, A., Balamurugan, K., Ponappa, K. & Kumar, B. M. Copper nanoparticles: Synthetic strategies, properties and multifunctional application. *Int. J. Nanosci.* **13**, 1430001. <https://doi.org/10.1142/s0219581x14300016> (2014).
76. Torabi, M., Fekri, L. Z. & Nikpassand, M. Synthesis, characterization and application of Fe₃O₄@ Silicapropyl@ vaniline-covalented isoniazid-copper (I) nanocomposite as a new, mild, effective and magnetically recoverable Lewis acid catalyst for the synthesis of acridines and novel azoacridines. *J. Mol. Struct.* **1250**, 131761 (2022).
77. Mohammadi, M. & Ghorbani-Choghamarani, A. Synthesis and characterization of novel hercynite@ sulfuric acid and its catalytic applications in the synthesis of polyhydroquinolines and 2, 3-dihydroquinazolin-4 (1 H)-ones. *RSC Adv.* **12**, 2770–2787 (2022).
78. Mohammadi, M. & Ghorbani-Choghamarani, A. Complexation of guanidino containing l-arginine with nickel on silica-modified Hercynite MNPs: a novel catalyst for the Hantzsch synthesis of polyhydroquinolines and 2,3-Dihydroquinazolin-4(1H)-ones. *Res. Chem. Intermed.* **48**, 2641–2663 (2022).
79. Lee, Y. & Hoveyda, A. H. Efficient boron–copper additions to aryl-substituted alkenes promoted by NHC-based catalysts enantioselective Cu-catalyzed hydroboration reactions. *J. Am. Chem. Soc.* **131**, 3160–3161 (2009).
80. Ton, N. N. H., Mai, B. K. & Nguyen, T. V. Tropylium-promoted hydroboration reactions: Mechanistic insights via experimental and computational studies. *J. Org. Chem.* **86**, 9117–9133 (2021).
81. Lillo, V. *et al.* Asymmetric β-boration of α, β-unsaturated esters with chiral (NHC) Cu catalysts. *Organometallics* **28**, 659–662 (2009).
82. Wei, C. & Li, C.-J. Enantioselective direct-addition of terminal alkynes to imines catalyzed by copper (I) pybox complex in water and in toluene. *J. Am. Chem. Soc.* **124**, 5638–5639 (2002).
83. Shah, S., Das, B. G. & Singh, V. K. Recent advancement in copper-catalyzed asymmetric reactions of alkynes. *Tetrahedron*, **93**, 132238 (2021).
84. Ghanbari, Z. & Naeimi, H. Tetrazol-Cu (i) immobilized on nickel ferrite catalyzed green synthesis of indenopyridopyrimidine derivatives in aqueous media. *RSC Adv.* **11**, 31377–31384 (2021).
85. Ghobakhloo, F., Azarifar, D., Mohammadi, M., Keypour, H. & Zeynali, H. Copper(II) Schiff-base complex modified UiO-66-NH₂ (Zr) metal-organic framework catalysts for Knoevenagel condensation-Michael addition–cyclization reactions. *Inorg. Chem.* **61**, 4825–4841 (2022).
86. Van Veldhuizen, J. J., Campbell, J. E., Giudici, R. E. & Hoveyda, A. H. A readily available chiral Ag-based N-heterocyclic carbene complex for use in efficient and highly enantioselective Ru-catalyzed olefin metathesis and Cu-catalyzed allylic alkylation reactions. *J. Am. Chem. Soc.* **127**, 6877–6882 (2005).
87. Sharghi, H., Ebrahimpourmoghaddam, S. & Doroodmand, M. M. Facile synthesis of 5-substituted-1H-tetrazoles and 1-substituted-1H-tetrazoles catalyzed by recyclable 4'-phenyl-2,2': 6',2''-terpyridine copper (II) complex immobilized onto activated multi-walled carbon nanotubes. *J. Organomet. Chem.* **738**, 41–48 (2013).
88. Tourani, H., Naimi-Jamal, M. R., Panahi, L. & Dekamin, M. G. Nanoporous metal-organic framework Cu₂(BDC)₂(DABCO) as an efficient heterogeneous catalyst for one-pot facile synthesis of 1, 2, 3-triazole derivatives in ethanol: Evaluating antimicrobial activity of the novel derivatives. *Scientia Iranica* **26**, 1485–1496. <https://doi.org/10.24200/sci.2018.50731.1841> (2019).
89. Tourani, H., Naimi-Jamal, M. R. & Dekamin, M. G. Preparation of 5-substituted-1H-tetrazoles catalyzed by MOFs via two strategies: Direct condensation of aryl nitriles with sodium azide, and tri-component reaction method. *ChemistrySelect* **3**, 8332–8337. <https://doi.org/10.1002/slct.201801392> (2018).
90. Sajjadifar, S., Zolfigol, M. A. & Chehardoli, G. Boron sulfuric acid as an efficient heterogeneous catalyst for the synthesis of 1-substituted 1H-1, 2, 3, 4-tetrazoles in polyethylene glycol. *Eurasian Chem Commun.* **2**, 812–818 (2020).
91. Koolivand, M., Nikoorazm, M., Ghorbani-Choghamarani, A. & Mohammadi, M. A novel cubic Zn-citric acid-based MOF as a highly efficient and reusable catalyst for the synthesis of pyranopyrazoles and 5-substituted 1H-tetrazoles. *Appl. Organomet. Chem.* **36**, e6656 (2022).
92. Patani, G. A. & LaVoie, E. J. Bioisosterism: A rational approach in drug design. *Chem. Rev.* **96**, 3147–3176 (1996).
93. Ornstein, P. L. *et al.* Structure–activity studies of 6-(tetrazolylalkyl)-substituted decahydroisoquinoline-3-carboxylic acid AMPA receptor antagonists. I. Effects of stereochemistry, chain length, and chain substitution. *J. Med. Chem.* **39**, 2219–2231 (1996).
94. Kees, K. L., Cheeseman, R. S., Prozialeck, D. H. & Steiner, K. E. Perfluoro-N-[4-(1H-tetrazol-5-ylmethyl) phenyl] alkanamides. A new class of oral antidiabetic agents. *J. Med. Chem.* **32**, 11–13 (1989).
95. Singh, H., Chawla, A. S., Kapoor, V. K., Paul, D. & Malhotra, R. K. 4 Medicinal chemistry of tetrazoles. *Prog. Med. Chem.* **17**, 151–183 (1980).
96. Bary, V., Conalty, M., O'Sullivan, J. & Twomey, D. Chemother., Chemother. In *Proc. 9th Int. Congr* Vol. 8, 103 (1977).
97. Okabayashi, T., Kano, H. & Makisumi, Y. Action of substituted azaindolizines on microorganisms. I. Action on lactic acid bacteria. *Chem. Pharm. Bull.* **8**, 157 (1960).
98. Molaei, S., Tamoradi, T., Ghadermazi, M. & Ghorbani-Choghamarani, A. Synthesis and characterization of MCM-41@ AMPD@ Zn as a novel and recoverable mesostructured catalyst for oxidation of sulfur containing compounds and synthesis of 5-substituted tetrazoles. *Microporous Mesoporous Mater.* **272**, 241–250 (2018).
99. Prasad, A. N., Reddy, B. M., Jeong, E.-Y. & Park, S.-E. Cu (II) PBS-bridged PMOs catalyzed one-pot synthesis of 1, 4-disubstituted 1, 2, 3-triazoles in water through click chemistry. *RSC Adv.* **4**, 29772–29781 (2014).
100. Jin, T., Kamijo, S. & Yamamoto, Y. Synthesis of 1-substituted tetrazoles via the acid-catalyzed [3+ 2] cycloaddition between isocyanides and trimethylsilyl azide. *Tetrahedron Lett.* **45**, 9435–9437 (2004).
101. Stierstorfer, J., Wurzenberger, M. H. H., Weippert, V. & Braun, V. Tailoring the properties of 3d transition metal complexes with different N-cycloalkyl-substituted tetrazoles. *New J. Chem.* **45**, 11042–11050 (2021).
102. Nasrollahzadeh, M., Nezafat, Z., Bidgoli, N. S. S. & Shafei, N. Use of tetrazoles in catalysis and energetic applications: Recent developments. *Mol. Catal.* **513**, 111788. <https://doi.org/10.1016/j.mcat.2021.111788> (2021).
103. Koguro, K., Oga, T., Mitsui, S. & Orita, R. Novel synthesis of 5-substituted tetrazoles from nitriles. *Synthesis* **1998**, 910–914 (1998).
104. Sauer, J., Huisgen, R. & Sturm, H. Zur acylierung von 5-aryl-tetrazolen; ein duplikationsverfahren zur darstellung von polyarylen. *Tetrahedron* **11**, 241–251 (1960).
105. Swami, S., Sahu, S. N. & Shrivastava, R. Nanomaterial catalyzed green synthesis of tetrazoles and its derivatives: A review on recent advancements. *RSC Adv.* **11**, 39058–39086. <https://doi.org/10.1039/D1RA05955F> (2021).

106. Heravi, M. M., Zadsirjan, V., Dehghani, M. & Ahmadi, T. Towards click chemistry: Multicomponent reactions via combinations of name reactions. *Tetrahedron* **74**, 3391–3457. <https://doi.org/10.1016/j.tet.2018.04.076> (2018).
107. El Anwar, S., Růžicková, Z., Baval, D., Fojt, L. & Grüner, B. Tetrazole ring substitution at carbon and boron sites of the cobalt bis(dicarbollide) ion available via dipolar cycloadditions. *Inorg. Chem.* **59**, 17430–17442. <https://doi.org/10.1021/acs.inorgchem.0c02719> (2020).
108. Mittal, R. & Awasthi, S. K. Recent advances in the synthesis of 5-substituted 1H-tetrazoles: A complete survey (2013–2018). *Synthesis* **51**, 3765–3783 (2019).
109. Shelkar, R., Singh, A. & Nagarkar, J. Amberlyst-15 catalyzed synthesis of 5-substituted 1-H-tetrazole via [3+2] cycloaddition of nitriles and sodium azide. *Tetrahedron Lett.* **54**, 106–109. <https://doi.org/10.1016/j.tetlet.2012.10.116> (2013).
110. Yuan, X., Wang, Z., Zhang, Q. & Luo, J. An intramolecular relay catalysis strategy for Knoevenagel condensation and 1,3-dipolar cycloaddition domino reactions. *RSC Adv.* **9**, 23614–23621. <https://doi.org/10.1039/C9RA04081A> (2019).
111. Matloubi Moghaddam, F., Eslami, M. & Ghadirian, N. MCM-41-SO₃H as an efficient reusable nano-ordered heterogeneous catalyst for the synthesis of divers 1- & 5-substituted 1H-tetrazoles. *Scientia Iranica* **26**, 1463–1473. <https://doi.org/10.24200/sci.2018.21088> (2019).
112. Kamijo, S. *et al.* Tetrazole synthesis via the palladium-catalyzed three component coupling reaction. *Mol. Divers.* **6**, 181–192. <https://doi.org/10.1023/B:MODI.0000006755.04495.d3> (2003).
113. Tisseh, Z. N., Dabiri, M., Nobahar, M., Khavasi, H. R. & Bazgir, A. Catalyst-free, aqueous and highly diastereoselective synthesis of new 5-substituted 1H-tetrazoles via a multi-component domino Knoevenagel condensation/1, 3 dipolar cycloaddition reaction. *Tetrahedron* **68**, 1769–1773 (2012).
114. Safapoor, S., Dekamin, M. G., Akbari, A. & Naimi-Jamal, M. R. Synthesis of (E)-2-(1H-tetrazole-5-yl)-3-phenylacrylonitrile derivatives catalyzed by new ZnO nanoparticles embedded in a thermally stable magnetic periodic mesoporous organosilica under green conditions. *Sci. Rep.* **12**, 10723. <https://doi.org/10.1038/s41598-022-13011-9> (2022).
115. Doustkhah, E. *et al.* Thiourea bridged periodic mesoporous organosilica with ultra-small Pd nanoparticles for coupling reactions. *RSC Adv.* **7**, 56306–56310 (2017).
116. Bing Liu, X., Liu, Y. & Lin Hu, Y. Highly active benzotriazolium ionic liquid-modified periodic mesoporous organosilica supported samarium/lanthanum nanoparticles for sustainable transformation of carbon dioxide to cyclic carbonates. *J. Mexican Chem. Soc.* **64**, 201–217 (2020).
117. Mardiansyah, D. *et al.* Effect of temperature on the oxidation of Cu nanowires and development of an easy to produce, oxidation-resistant transparent conducting electrode using a PEDOT:PSS coating. *Sci. Rep.* **8**, 10639. <https://doi.org/10.1038/s41598-018-28744-9> (2018).
118. Hajizadeh, Z., Hassanzadeh-Afrouzi, F., Jelodar, D. F., Ahghari, M. R. & Maleki, A. Cu (II) immobilized on Fe₃O₄@HNTs–tetrazole (CFHT) nanocomposite: Synthesis, characterization, investigation of its catalytic role for the 1, 3 dipolar cycloaddition reaction, and antibacterial activity. *RSC Adv.* **10**, 26467–26478 (2020).
119. Akbarzadeh, P., Koukabi, N. & Kolvari, E. Three-component solvent-free synthesis of 5-substituted-1H-tetrazoles catalyzed by unmodified nanomagnetite with microwave irradiation or conventional heating. *Res. Chem. Intermed.* **45**, 1009–1024 (2019).
120. Bakherad, M., Doosti, R., Keivanloo, A., Gholizadeh, M. & Jadidi, K. Rapid, green, and catalyst-free one-pot three-component syntheses of 5-substituted 1H-tetrazoles in magnetized water. *J. Iran. Chem. Soc.* **14**, 2591–2597 (2017).
121. Ostrovskii, V. A., Popova, E. A. & Trifonov, R. E. In *Comprehensive Heterocyclic Chemistry IV* (eds Black, D. S. C. *et al.*) 182–232 (Elsevier, 2022).
122. Safaei-Ghomi, J. & Paymard-Samani, S. Facile and rapid synthesis of 5-substituted 1H-tetrazoles via a multicomponent domino reaction using nickel (II) oxide nanoparticles as catalyst. *Chem. Heterocycl. Compd.* **50**, 1567–1574 (2015).
123. Taghavi, F., Gholizadeh, M., Saljooghi, A. S. & Ramezani, M. Cu (ii) immobilized on Fe₃O₄@APTMS-DFX nanoparticles: An efficient catalyst for the synthesis of 5-substituted 1 H-tetrazoles with cytotoxic activity. *MedChemComm* **8**, 1953–1964 (2017).
124. Abdollahi-Alibeik, M. & Moaddeli, A. Multi-component one-pot reaction of aldehyde, hydroxylamine and sodium azide catalyzed by Cu-MCM-41 nanoparticles: A novel method for the synthesis of 5-substituted 1 H-tetrazole derivatives. *New J. Chem.* **39**, 2116–2122 (2015).
125. Lang, L., Zhou, H., Xue, M., Wang, X. & Xu, Z. Mesoporous ZnS hollow spheres-catalyzed synthesis of 5-substituted 1H-tetrazoles. *Mater. Lett.* **106**, 443–446 (2013).

Acknowledgements

We are grateful for the financial support from The Research Council of Iran University of Science and Technology (IUST), Tehran, Iran (Grant No 160/20969) for their support. We would also like to acknowledge the support of The Iran Nanotechnology Initiative Council (INIC), Iran.

Author contributions

(1) E.V. worked on the topic as his Ph.D thesis and prepared the initial draft of the manuscript.(2) M.G.D. is the supervisor of E.V. Also, he edited and revised the manuscript completely.

Competing interests

The authors declare no competing interests.

Additional information

Supplementary Information The online version contains supplementary material available at <https://doi.org/10.1038/s41598-022-22905-7>.

Correspondence and requests for materials should be addressed to M.G.D.

Reprints and permissions information is available at www.nature.com/reprints.

Publisher's note Springer Nature remains neutral with regard to jurisdictional claims in published maps and institutional affiliations.



Open Access This article is licensed under a Creative Commons Attribution 4.0 International License, which permits use, sharing, adaptation, distribution and reproduction in any medium or format, as long as you give appropriate credit to the original author(s) and the source, provide a link to the Creative Commons licence, and indicate if changes were made. The images or other third party material in this article are included in the article's Creative Commons licence, unless indicated otherwise in a credit line to the material. If material is not included in the article's Creative Commons licence and your intended use is not permitted by statutory regulation or exceeds the permitted use, you will need to obtain permission directly from the copyright holder. To view a copy of this licence, visit <http://creativecommons.org/licenses/by/4.0/>.

© The Author(s) 2022